

Using the Continuous Spectrum to “Feel” Integrability: the Effect of Boundary Conditions

Panayotis G. Kevrekidis[†] and Niurka R. Quintero[‡]

[†]*Department of Mathematics and Statistics, University of Massachusetts, Amherst MA 01003-4515, USA;*

[‡]*Departamento de Física Aplicada I, Escuela Universitaria Politécnica, Universidad de Sevilla, Virgen de África 7, 41011, Sevilla, Spain; and Instituto CARLOS I de Física Teórica y Computacional Universidad de Granada. E-18071 Granada, Spain*

The scope of this work is to propose a method for testing the integrability of a model partial differential (PDE) and/or differential difference equation (DDE). For monoparametric families of PDE/DDE’s, that are known to possess isolated integrable points, we find that very special features occur in the continuous (“phonon”) spectrum at these “singular” points. We identify these features in the case example of a PDE and a DDE (that sustain front and pulse-like solutions respectively) for different types of boundary conditions. The key finding of the work is that such spectral features are generic near the singular, integrable points and hence we propose to explore a given PDE/DDE for such traits, as a means of assessing its potential integrability.

Integrable models of partial differential (PDE) and differential difference (DDE) equations have been a topic of intense investigation over the past few decades [1–3]. The main reason for that, except for the wide variety of physical applications that can be described by integrable or near-integrable systems, is that the special case of integrable models can be analyzed completely by means of the inverse scattering transform [1,4]. This can then serve as a starting point for perturbative treatment of near-integrable systems.

In the process of these developments, a number of techniques have been developed for assessing integrability in continuous [5] or discrete [6] settings (or applicable to both [7]). An interesting feature of these “tests” is that they are necessary (but not sufficient) conditions for integrability. Hence, if a model equation fails such a criterion, it is non-integrable, but if it passes, it may or *may not* be integrable. In a sense, this suggests that we still do not understand the *essential ingredients* that render a system completely integrable. Of course, should a Lax pair be identified and the inverse scattering mechanism be applied, we know that the system is integrable, but it would certainly be desirable (as is clear from all the above effort to create “integrability tests”) to have a mechanistic (“black box”) type of criterion to assess that.

We, of course, do not claim to be providing a full answer to this question in the present work. However, we will try to give a number of useful hints that may lead to partial answers to the above questions and may provide some new intuition in the effort to construct such mechanistic criteria.

Our tool of choice will be the use of different sets of boundary conditions (BC) to “feel” the continuous spectrum (CS) of the linearization around the nonlinear coherent structure that the PDE/DDE of interest supports. Notice that the effect of boundary conditions in related contexts has been studied in a number of references; see e.g., [8] and references therein. However, in all of these works the effects of the BC to the point spectrum (rather than the CS) were assessed and moreover this was not done in direct connection with issues of integrability.

In the present work, we focus on two model problems, to establish our findings and demonstrate their generality. The models are selected as one parameter families of equations such that one member of the family is an integrable system. Moreover, in illustrating the generality of the conclusions, they are selected in a form such that the one model corresponds to a PDE, while the other to a DDE and so that the one is kink bearing, while the other is pulse bearing. The models of interest will be the parametrically modified sine-Gordon equation (often also called the Peyrard-Remoissenet (PR) model) [9] and a modified version of the discrete nonlinear Schrödinger (DNLS) model (occasionally called the Salerno model) [10]. The former PDE reads:

$$\phi_{tt} - \phi_{xx} = -\frac{dU}{d\phi}, \quad U(\phi, r) = \frac{(1-r)^2 [1 - \cos(\phi)]}{1 + r^2 + 2r \cos(\phi)}, \quad |r| < 1, \quad |x| < \infty, \quad (1)$$

while the latter DDE is of the form:

$$i\dot{u}_n = -\Delta_2 u_n - |u_n|^2 [2\epsilon u_n + (1 - \epsilon)(u_{n+1} + u_{n-1})]. \quad (2)$$

The most well-known among these monoparametric families of models are the sine-Gordon equation (Eq. (1), for $r = 0$) which is relevant to superconductivity and charge density waves among other applications [2] and the experimentally realizable discrete nonlinear Schrödinger equation [11] of $\epsilon = 1$, as well as its integrable, so-called Ablowitz-Ladik [12] counterpart for $\epsilon = 0$ in the case of Eq. (2).

Notice that for the PDE, the subscripts denote partial derivatives of the field, while for the DDE, the overdot denotes temporal derivative, $\Delta_2 u_n \equiv C(u_{n+1} - 2u_n + u_{n-1})$ where $C = 1/(\Delta x)^2$ is a constant determined by the

lattice spacing Δx ; the subscript n denotes the lattice site index. In the former case, there exist kink-like solutions which have been detailed in [9], while in the latter, the field is complex and there exist pulse-like solutions of the form $u_n = \exp(i\Lambda t)v_n$, where Λ is the frequency of the solutions and v_n its (real) exponentially localized spatial profile [10,11].

In the PDE, linearization around a state $\phi_0(x)$, using the ansatz $\phi_0(x) + \delta \exp(i\omega t)f(x)$ into Eq. (1), yields to $O(\delta)$ the linearization equation

$$f_{xx} + \left(\omega^2 - \frac{(r^2 - 1)^2 [(r^2 + 1) \cos[\phi_0(x)] + r(3 - \cos[2\phi_0(x)])]}{[1 + r^2 + 2r \cos(\phi_0(x))]^3} \right) f = 0, \quad |x| < \infty. \quad (3)$$

Notice that when $r = 0$, $\phi_0(x) = 4 \arctan[\exp(x)]$ (static kink solution of the sG equation) and for this function, the Sturm-Liouville problem (3) can be exactly solved [13] yielding one discrete mode (Goldstone mode) at $\omega = 0$ and the continuous spectrum represented by the phonons. For $r \neq 0$, neither the static solution nor the linearization spectrum are explicitly available. Hence, to investigate the linear spectrum of Eq. (3), we should find its numerical solution, by discretizing the equation in a numerical mesh for a finite domain. The mesh consists of the $N + 1$ points $x_j = \{-L/2 + j\Delta x; \quad j = 0, 1, 2, \dots, N\}$ defined in the finite length L of the system ($\Delta x = L/N$). Notice that since, in this case, we wish to emulate the behavior of the PDE, Δx is very fine (typically 0.05), and the robustness of the findings upon variation of the (small) Δx has been verified.

When we compute the solution either of the PDE or of the linearization equation, we consider three different types of BC. Free BC are expressed through $f(0) = f(1)$ and $f(N) = f(N - 1)$ (notice that $f(j) = f(x_j)$). Fixed BC are given by $f(0) = 0$ and $f(N) = 0$, while (anti-)periodic BC are given by $f(0) = -f(N - 1)$ and $f(N) = -f(1)$.

Analogously to the PDE, for the linear stability analysis of DDE (2) we insert $\exp(i\Lambda t)[v_n + \delta(U_n e^{-i\omega t} + W_n e^{i\omega^* t})]$ into Eq. (2). We thus obtain to order $O(\delta)$ the following eigenvalue problem for $\{\omega, \{U_n, W_n^*\}\}$

$$\omega \begin{pmatrix} U_n \\ W_n^* \end{pmatrix} = \mathcal{L} \begin{pmatrix} U_n \\ W_n^* \end{pmatrix}, \quad \mathcal{L} = \begin{pmatrix} A & B \\ -B & -A \end{pmatrix}, \quad (4)$$

$$A_{mn} = [\Lambda + 2C - (4\epsilon v_n^2 + (1 - \epsilon)v_n[v_{n+1} + v_{n-1}])]\delta_{m,n} + [(1 - \epsilon)v_n^2 - C](\delta_{m,n+1} + \delta_{m,n-1}),$$

$$B_{mn} = -v_n[2\epsilon v_n + (1 - \epsilon)(v_{n+1} + v_{n-1})]\delta_{m,n},$$

where the stars denote complex conjugation. We compute the solutions of DDE (2) and Eq. (4) using 200 points, $\Delta x = 0.75$. The BC are defined analogously through $U_0 = U_1$, $U_N = U_{N-1}$, $W_0 = W_1$, and $W_N = W_{N-1}$ for free BC. For fixed BC: $U_0 = 0$, $U_N = 0$, $W_0 = 0$, and $W_N = 0$, while for periodic BC: $U_0 = U_{N-1}$, $U_N = U_1$, $W_0 = W_{N-1}$, and $W_N = W_1$.

We have also tried no-flux boundary conditions that yield essentially the same results as in the free BC case.

Our results when the parameter of the PR potential or ϵ in the DDE are varied can be summarized in Figs. 1-3.

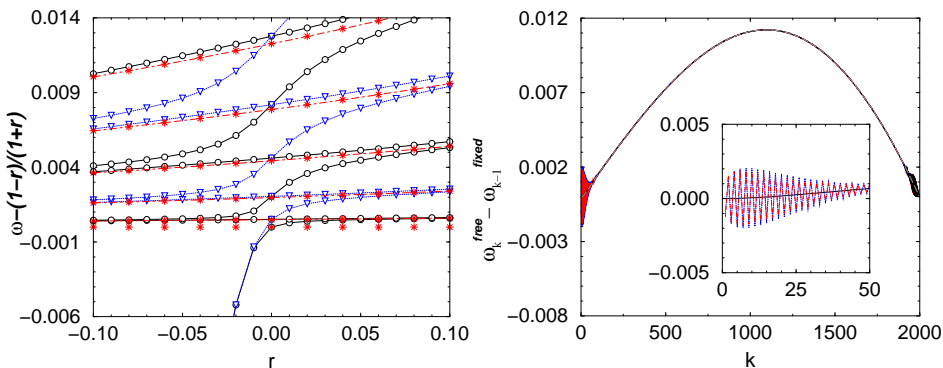


FIG. 1. Comparison (left subplot) of the eigenfrequencies of linear spectrum for fixed and free BC: We have plotted the difference between the eigenfrequencies computed from the Eq. (3) and $\omega_{min} = (1 - r)/(1 + r)$ versus r . The circles joined by solid line (free BC) represent how far the frequencies are from the lower phonon mode. The triangles joined by dotted lines correspond to fixed BC. Here, we have also added the distribution of the eigenfrequencies when we linearize around the zero solution by using stars (free BC) and dot-dashed line (fixed). The difference between the frequencies for free and fixed BC, $\omega_k^{free} - \omega_k^{fixed}$ ($2 \leq k \leq N - 1$), is plotted in the right subplot as a function of the wave number for $r = 0$ (solid line), $r = -0.02$ (dashed line) and $r = 0.02$ (dotted line). We observe an oscillatory behaviour for the last wave numbers (in the inset the same difference is shown for the first wave numbers). For the linear PR case, the results essentially coincide with the integrable nonlinear case of $r = 0$ (solid line).

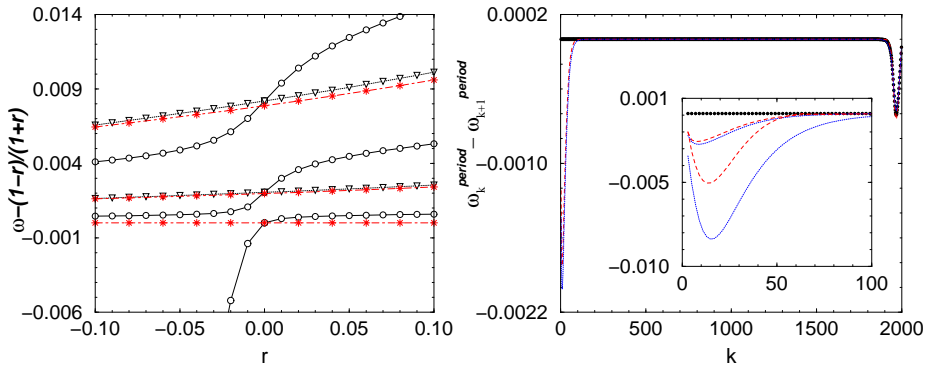


FIG. 2. Periodic BC: The left panel shows the difference between the numerical eigenfrequencies computed from Eq. (3), and ω_{min} versus r . The frequencies corresponding to the spectrum of the linear PR case are also shown by stars for free BC and dot-dashed line for the fixed BC case. In the right panel we show the difference between $\omega_k^{period} - \omega_{k+1}^{period}$ versus k ($k = 2, 4, \dots, N - 2$). The stars practically at zero for all k represent the integrable system ($r = 0$), whereas the dashed ($r = -0.02$) and dotted ($r = 0.02$) lines correspond to non-integrable cases. In the inset we observe that the difference between these frequencies increases as r increases (the case of $r = -0.1$ (dashed line) and $r = 0.1$ (dotted line) are also included).

From the above results the following conclusions can be drawn:

1. For fixed BC, the CS band edge frequency is prohibited. Hence, we compare ω_k^{free} with ω_{k-1}^{fixed} . We find that for small wavenumbers, fixed and free BC eigenfrequencies practically coincide *only* in the integrable case, whereas for the non-integrable case we observe an oscillatory behaviour of this function.
2. For periodic BC, the CS comprises of modes coming alternately from the free and fixed BC. This seems natural as the free boundary conditions select eigenmodes symmetric at the boundary, the fixed ones select modes antisymmetric at the boundary, while the periodic BC allow for both.
3. An additional feature, equally important as 1. (especially in view of its potential predictive power) is the fact that for the integrable case of $r = 0$, periodic BC essentially imply the presence of *double* eigenvalues. The difference between the two eigenvalues is of the $O(10^{-9})$ for all pairs (except for the cutoff, discretization induced phenomena at the upper end of the spectrum). This is in sharp contrast (in particular for small wavenumbers), to even mild breakings of integrability, as can be inferred from Fig. 2.
4. Statements 1. and 3. above can be used in predictive form and constitute the criterion (algorithm) set forth in this work: for a given PDE/DDE model, find the steady state coherent structure (e.g., by finding the exact solution of an ODE, or numerically performing a Newton type algorithm). Linearize around the exact solution and study, in particular, the small wavenumbers, close to the lower edge of the CS (we assume that the problem is monoparametric in what follows, but it is clear that the application of the criterion does not require that). If for a critical/singular value of the parameter the fixed BC and free BC (small k) eigenvalue spectra essentially coincide and the multiplicity of periodic BC eigenvalues becomes double, then the model for this unique value of the parameter can be “strongly suspected” to be integrable. We use the above expression, as we provide no rigorous proof, but only supporting (but rather universal in distinct models with distinct features/solutions) numerical evidence for this statement.

5. We now attempt to give a *qualitative explanation* for the criterion set forth. One can solve explicitly (by means of Chebyshev polynomials) the discretized linearization problem of the PR model, to find: $\omega_{k+1}^{free} = \sqrt{\omega_{min}^2 + (4/(\Delta x)^2) \sin^2(k\pi/(2N-2))}$, $k = 0, 1, \dots, N-2$; for fixed BC $\omega_k^{fixed} = \sqrt{\omega_{min}^2 + (4/(\Delta x)^2) \sin^2(k\pi/(2N))}$, $k = 1, 2, \dots, N-1$; for periodic BC $\omega_0 = \omega_{min}$, $\omega_k = \sqrt{\omega_{min}^2 + (4/(\Delta x)^2) \sin^2(k\pi/(N-1))}$, $\omega_{N-1-k} = \omega_k$, $k = 1, \dots, (N-2)/2$, respectively. From the above expressions, $\omega_k^{free} \approx \omega_{k-1}^{fixed}$ for small k . The difference between these two sets of frequencies as a function of k practically does not depend on r and coincides with the spectrum for the nonlinear integrable case $r = 0$, except for the oscillatory behavior at the edge. For periodic BC, except for the first phonon frequency, $\omega_{k+1} = \omega_{N-2-k}$, all the eigenfrequencies are of algebraic multiplicity 2. In both situations (for fixed-free and for periodic BC), the linearization around the nonlinear wave (kink) shows the *exact same features* as the linearization around the uniform steady state *only in the integrable case*. That is because, it is only in that case, that the potential is *reflectionless* [1,4] and, hence, there is no reflection in the scattering from the nonlinear wave. Such a reflection would lead to an eigenfrequency adjustment in the non-integrable case (in order to satisfy the boundary value eigenvalue problem). However, it is only for the integrable case that the CS (used here to “perceive” the presence of the nonlinear wave

through the scattering) will not “feel” the wave (as only in this singular case there is no reflection from it).

7. We have also tested the validity of these results also in equation (2), in the vicinity of the integrable limit $\epsilon = 0$, with similar conclusions. For brevity, we only show the case of periodic BC. In Fig. 3, it can be clearly seen that it is only for the integrable case that the double eigenvalue multiplicity is obtained.

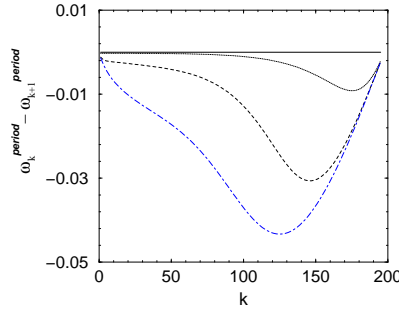


FIG. 3. Periodic BC for AL-DNLS: The solid line at zero represents the difference between two consecutive frequencies ($k = 2, 4, \dots$) for the integrable A-L lattice ($\epsilon = 0$). The double multiplicity of the frequencies is destroyed as ϵ is increased (dotted, dashed and dot-dashed lines represent the non-integrable cases of $\epsilon = 0.1, 0.5, 1$ respectively).

In conclusion, we have proposed and used a new test for revealing the potential integrable nature of a given model problem. By varying the boundary conditions and “feeling” the effects of such variations in the CS, we have revealed that the small wavenumbers (particularly, but also the CS more generally) have singular ways of responding to the unique parameter values for which the model is integrable. These singular features (such as an approximate identification of fixed with free BC, small k eigenvalues and the double multiplicity of eigenvalues for periodic BC) can be used to identify and single out the integrable behavior. We have provided two model examples respectively for kinks and pulses and for a PDE and a DDE. Independently of the detailed structure of the model these properties have been identified as universal. It is naturally interesting to explore the potential usefulness of such a criterion in various more complex settings. It would also be of value to rigorously elucidate the mathematical structure that underlies the findings presented herein (we have only qualitatively attempted to justify this structure here).

- [1] M.J. Ablowitz and H. Segur, *Solitons and the Inverse Scattering Transform* (SIAM, Philadelphia, 1981).
- [2] R.K. Dodd, J.C. Eilbeck, J.D. Gibbon, and H.C. Morris *Solitons and Nonlinear Wave Equations* (Academic Press, London, 1982).
- [3] A. C. Scott, *Nonlinear Science* (Oxford University Press, 1999).
- [4] L.D. Faddeev, L.A. Takhtajan, *Hamiltonian methods in the theory of solitons* (Berlin ; New York : Springer-Verlag, 1987).
- [5] P. Painlevé, C.R. Acad. Sci. (Paris) **130**, 1112 (1900); A. Ramani, B. Grammaticos and A. Bountis, Phys. Rep. **180**, 159 (1989); R. Conte solv-int/9710020.
- [6] B. Grammaticos, A. Ramani and V. Papageorgiou, Phys. Rev. Lett. **67**, 1825 (1991); A. Ramani, B. Grammaticos and J. Hietarinta, Phys. Rev. Lett. **67**, 1829 (1991); M. Bellon and C.-M. Viallet, chao-dyn/9805006; J. Hietarinta and C. Viallet, Phys. Rev. Lett. **81**, 325 (1998).
- [7] P.G. Kevrekidis, Phys. Lett. A **285**, 383 (2001).
- [8] R. M. DeLeonardis, S. E. Trullinger, and R. F. Wallis, J. Appl. Phys. **51**, 1211 (1211); P.G. Kevrekidis, I.G. Kevrekidis and B.A. Malomed, J. Phys. A **35** 267 (2002); K.Ø. Rasmussen, D. Cai, A.R. Bishop and N. Grønbech-Jensen, Phys. Rev. E **55**, 6151 (1997).
- [9] M. Remoissenet and M. Peyrard, J. Phys. C: Solid State Phys. **14**, L481, (1981); M. Peyrard and M. Remoissenet Phys. Rev. B **26**, 2886 (1982); see also Niurka R. Quintero and Panayotis G. Kevrekidis, Physica D **170**, 31, (2002).
- [10] D. Cai, A. R. Bishop, and N. Grønbech-Jensen, Phys. Rev. Lett. **72**, 591 (1994).
- [11] see e.g., P.G. Kevrekidis, K.Ø. Rasmussen and A.R. Bishop, Intn. J. Mod. Phys. B **15**, 2833 (2001) and references therein.
- [12] M.J. Ablowitz and J.F. Ladik, J. Math. Phys. **16**, 598 (1975); *ibid.* **17**, 1011 (1976).
- [13] Julio Rubinstein, Journal of Math. Phys. **11**, 258, (1970).